



**HAL**  
open science

# A Water-Soluble Peptoid Chelator that Can Remove Cu<sup>2+</sup> from Amyloid- $\beta$ Peptides and Stop the Formation of Reactive Oxygen Species Associated with Alzheimer's Disease

Anastasia E Behar, Laurent Sabater, Maria Baskin, Christelle Hureau, Galia Maayan

## ► To cite this version:

Anastasia E Behar, Laurent Sabater, Maria Baskin, Christelle Hureau, Galia Maayan. A Water-Soluble Peptoid Chelator that Can Remove Cu<sup>2+</sup> from Amyloid- $\beta$  Peptides and Stop the Formation of Reactive Oxygen Species Associated with Alzheimer's Disease. *Angewandte Chemie International Edition*, 2021, 60 (46), pp.24588-24597. 10.1002/anie.202109758 . hal-03395343

**HAL Id: hal-03395343**

**<https://hal.science/hal-03395343>**

Submitted on 22 Oct 2021

**HAL** is a multi-disciplinary open access archive for the deposit and dissemination of scientific research documents, whether they are published or not. The documents may come from teaching and research institutions in France or abroad, or from public or private research centers.

L'archive ouverte pluridisciplinaire **HAL**, est destinée au dépôt et à la diffusion de documents scientifiques de niveau recherche, publiés ou non, émanant des établissements d'enseignement et de recherche français ou étrangers, des laboratoires publics ou privés.

# A Water-Soluble Peptoid Chelator that Can Remove Cu<sup>2+</sup> from Amyloid- $\beta$ and Stop the Formation of Reactive Oxygen Species Associated with Alzheimer's Disease

Anastasia E. Behar<sup>[a]</sup>, Laurent Sabater<sup>[b]</sup>, Maria Baskin<sup>[a]</sup>, Christelle Hureau<sup>\*[b]</sup> and Galia Maayan<sup>\*[a]</sup>

[a] A.E. Behar, Dr. M. Baskin, Prof. Dr. G. Maayan  
Schulich Faculty of Chemistry  
Technion – Israel Institute of Technology  
Technion City, 3200008 Haifa (Israel)  
E-mail: gm92@technion.ac.il

[b] Dr. L. Sabater, Prof. Dr. C. Hureau,  
CNRS; LCC (Laboratoire de Chimie de Coordination)  
205 route de Narbonne, 31077 Toulouse (France)  
and  
Université de Toulouse  
31077 Toulouse (France)  
E-mail: christelle.hureau@lcc-toulouse.fr

Supporting information for this article is given via a link at the end of the document.

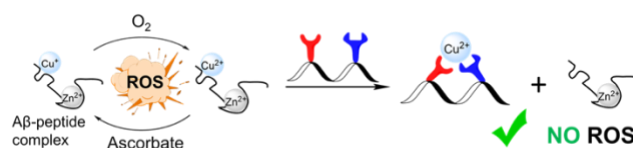
**Abstract:** Cu bound to Amyloid- $\beta$  (A $\beta$ ) peptides can act as a catalyst for the formation of reactive oxygen species (ROS), leading to neuropathologic degradation associated with Alzheimer's disease (AD). An excellent therapeutic approach is to use a chelator that can selectively remove Cu from Cu-A $\beta$ . This chelator should compete with Zn<sup>2+</sup> ions (Zn) that are present in the synaptic cleft while forming a nontoxic Cu complex. Herein we describe **P3**, a water-soluble peptidomimetic chelator that selectively removes Cu(II) from Cu-A $\beta$  in the presence of Zn and prevent the formation of ROS even in a reductive environment. We demonstrate, based on extensive spectroscopic analysis, that although **P3** extracts Zn from Cu,Zn-A $\beta$  faster than in removes Cu, the formed Zn complexes are kinetic products that further dissociate, while Cu**P3** is formed as an exclusive stable thermodynamic product. Our unique findings, combined with the bioavailability of peptoids, make **P3** an excellent drug candidate in the context of AD.

## 1. Introduction

Copper ions are key elements in the structure and function of natural biopolymers<sup>[1]</sup>, however, their overloading can be potentially toxic to living cells and may cause oxidative stress, cardiovascular disorders and neurodegenerative diseases including Alzheimer's disease (AD).<sup>[2]</sup> A known approach towards the development of therapeutics for AD is Cu-chelation.<sup>[3]</sup> The amyloid cascade hypothesis proposes that copper ions (Cu) play a harmful role in the excessive accumulation of a peptide called amyloid- $\beta$  (A $\beta$ ),<sup>[4]</sup> which is associated with AD. In addition, it was previously shown that Cu-A $\beta$  complex can catalyze the incomplete reduction of dioxygen by ascorbate as a reduction agent, leading to formation of reactive oxygen species (ROS), namely, superoxide O<sub>2</sub><sup>-</sup>, hydrogen peroxide H<sub>2</sub>O<sub>2</sub> or hydroxyl radical HO<sup>•</sup>.<sup>[3c]</sup> Therefore, removal of Cu-ions from Cu-A $\beta$  complex could be one of the possible therapeutic approaches to prevent this process.<sup>[5]</sup> However, an important prerequisite for any chelator for Cu in context of AD, is not only the ability to compete with A $\beta$  on Cu binding in order to prevent Cu-A $\beta$  complex from catalyzing the production of ROS, but also to form a new Cu-

chelator complex that is unable to catalyze formation of ROS on its own.<sup>[3b]</sup>

Although Zn<sup>2+</sup> ions do not lead to the production of ROS, their concentration in the synaptic cleft is higher than the concentration of Cu,<sup>[6]</sup> making them more available for coordination than Cu. Moreover, as the A $\beta$  affinity to Zn<sup>2+</sup> is relatively lower than its affinity to Cu (at neutral pH,  $K_A(\text{Zn}^{2+}\text{-A}\beta) = 10^5 - 10^6 \text{ M}^{-1}$  [3d, 7],  $K_A(\text{Cu}^{2+}\text{-A}\beta) = 10^{9-10} \text{ M}^{-1}$  [8] and  $K_A(\text{Cu}^+\text{-A}\beta) = 10^{7-10} \text{ M}^{-1}$  [9]), it is possible that the examined Cu chelator will extract the Zn<sup>2+</sup> ions from A $\beta$  rather than extracting the Cu<sup>2+</sup> ions from the toxic Cu-A $\beta$  complex, thus hindering the inhibition of ROS production.<sup>[3b, 10]</sup> Therefore, an ideal candidate for copper chelating towards the development of potential therapeutics for AD, should: (i) have an affinity towards Cu, which is high enough in order to extract Cu from Cu-A $\beta$  but not too high to withdraw Cu from other essential metalloproteins,<sup>[3b, 5e-f, 9, 11]</sup> (ii) have high selectivity to Cu over Zn<sup>[3b, 10]</sup>, and (iii) not lead to the production of ROS (Scheme 1).<sup>[3b]</sup>



**Scheme 1.** Representation of a metal chelator designed to selectively extract Cu ions from A $\beta$  peptide complex, associated with ROS production in the context of AD.

Although the usefulness of targeting Cu in the context of AD was questioned,<sup>[12]</sup> with the strongest argument being that none of the promising ligands studied in vitro show any clinical benefit, the criteria to be fulfilled by the chelators are continuously refined,<sup>[3b]</sup> while improvement of the chelators is nurtured by in vitro studies<sup>[13, 14]</sup>. Despite a growing number of studies reporting on new Cu chelators, many challenges remain in order for these chelators to be developed as efficient drugs.<sup>[3b]</sup> This is because such chelators should meet several requirements including appropriate affinity and selectivity towards the targeted metal ion(s), good kinetic and stability properties, redox inertness together with BBB permeability and low toxicity.<sup>[3b]</sup> Small molecules Cu chelators, for example, are usually highly toxic, lead

## RESEARCH ARTICLE

to a wide range of side effects, are unable to cross cell membranes and can only reach their target in the extracellular regions.<sup>[15]</sup> Peptide-based drugs can overcome some of these problems, but have other disadvantages: they typically show low blood-brain barrier (BBB) penetrability due to their large size, polarity and large number of hydrogen bond donors/acceptors, have short half-lives as well as low bioavailability, and they exhibit proteolytic instability and rapid clearance.<sup>[16]</sup> Thus, it is desirable to develop a unique type of chelators, preferably peptidomimetic-based ones that can combine the advantages of both small molecules and peptide-based drug candidates.

Peptoids<sup>[17]</sup> – *N*-Substituted glycine oligomers – are excellent candidates for the development of metal chelators as potential therapeutics for AD: they can be easily synthesized on a solid support by the submonomer approach,<sup>[18]</sup> which utilizes primary amines as building blocks and thus allows to introduce a variety of functional groups within the peptoid sequence,<sup>[19]</sup> they are able to fold into well-defined secondary structures in solution,<sup>[20]</sup> and could be employed in various biological activities including protein-protein interactions,<sup>[21]</sup> metal binding and recognition<sup>[22]</sup>, and catalysis.<sup>[23]</sup> Moreover, compared to peptides, peptoids exhibit high proteolytic resistance<sup>[24]</sup> and high membrane permeability,<sup>[16a]</sup> together with tolerance towards high salts concentration and various pH conditions. In addition, some studies on the application of peptoids (not as chelators) towards AD therapy were previously reported and these were focused on inhibiting A $\beta$ -peptide aggregation rather than on the arrest of ROS production.<sup>[25]</sup>

We have recently described the helical peptoid chelator **Helix HQT i +3 (P1)**, Fig. 1A), which is a hexamer incorporating a 8-hydroxyquinoline (HQ) group and a 2,2':6',2''-Terpyridine (Terpy) group at the 2<sup>nd</sup> and 5<sup>th</sup> positions, and (S)-(+)-1-phenylethylamine (Nspe) groups at the other positions.<sup>[26]</sup> **P1** shows high selectivity to Cu<sup>2+</sup>, and can extract it from a methanolic solution containing 20 folds of similar metal ions such as Zn<sup>2+</sup> and Co<sup>2+</sup>.<sup>[26]</sup> We found that a primary request for this exceptional selectivity is the helicity of the peptoid with the two binding groups placed on the same side of the helix. The helical structure of **P1** was maintained via the four bulky chiral Nspe groups incorporated in addition within its sequence.<sup>[26]</sup> As a result, **P1** is hydrophobic and water insoluble, properties that limit its utilization as a drug candidate, despite its selectivity to Cu<sup>2+</sup>. Interestingly, we have recently shown that the incorporation of one or more piperazine units within the backbone of hydrophobic peptoids ensures their water-solubility, while maintaining their sequence and structure.<sup>[27]</sup> Capitalizing on these findings, we present here a new, water-soluble and helical peptoid chelator, which is selective for Cu<sup>2+</sup>, and describe how we applied it for the removal of Cu<sup>2+</sup> from A $\beta$  peptides, in aqueous medium, in order to stop the formation of ROS associated with AD, including in presence of Zn<sup>2+</sup>.

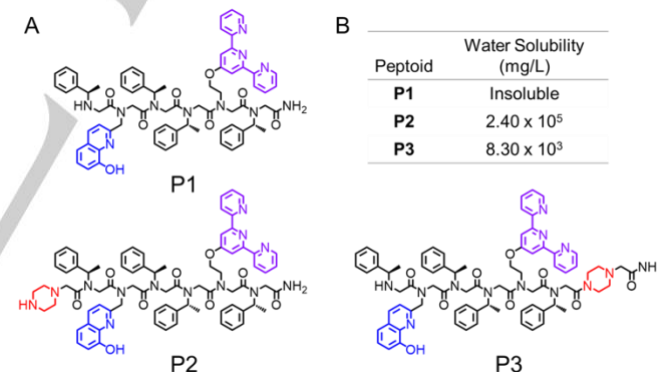
## 2. Results and Discussion

### 2.1 Synthesis and selectivity of water-soluble hydrophobic peptoid chelator

Our first goal was to explore whether our highly selective peptoid chelator described above (**Helix HQT i +3** or **P1**, Fig. 1A), which is insoluble in water, can become water-soluble upon the addition of one or two piperazine groups at the N- or C-terminals of its sequence while maintaining its selectivity to Cu<sup>2+</sup> in water.

To this aim, we have synthesized two peptoids based on **P1**, by incorporating only one piperazine group at either its N- or C-terminus, forming **P2** and **P3**, respectively (Fig. 1A and Fig. S1 to S6). Circular dichroism (CD) measurements of both peptoids in water resulted in spectra that exhibit double minima near 208 and 220 nm, characteristic of Nspe-based peptoid helix, indicating that both peptoids preserve their helical secondary structure in water (Fig. S7). In order to evaluate the selectivity of **P2** and **P3** towards Cu<sup>2+</sup> from a mixture solution containing 1 equiv. of Cu<sup>2+</sup> ions and 1 equiv. of the metal ions Co<sup>2+</sup>, Zn<sup>2+</sup>, Fe<sup>3+</sup>, Mn<sup>2+</sup> and Ni<sup>2+</sup>, 1 equiv. of this mixture was added to 1 equiv. of each peptoid in unbuffered water and the UV-Vis spectra was recorded. The obtained UV-Vis spectrum in the case of **P2** was different from the spectrum of its copper complex (Fig. S8, left) suggesting that there is no selective binding to Cu<sup>2+</sup> by **P2**.<sup>[26]</sup> In contrast, the UV-Vis spectrum obtained in the case of **P3** was identical to the spectrum of its copper complex (Fig. S8, right) implying a selective binding in this case. This selective binding was further supported by MS studies of solutions containing either **P3** and Cu or **P3** with a mixture of metal ions (Fig. S9-13). These apparent conflicting results may be attributed to the ability of piperazine, when incorporated at the N-terminus, to participate in the binding of some metal ions and disable the unique coordination geometry of the Cu<sup>2+</sup> complex that allows its selective binding.<sup>[26]</sup> Therefore, we can conclude that the addition of one piperazine group at the C-terminus of **P1**, leads to its water-soluble analogue **P3**, while maintaining both the hydrophobic sequence of **P1**, its helical structure and its fairly high selectivity to Cu<sup>2+</sup>, but this time in aqueous solution.

**Figure 1.** Selective binding of Cu<sup>2+</sup> in water: (A) sequences of peptoid chelators



**P1-P3.** (B) Water solubility data for **P1-P3** at pH = 7.0

### 2.2 Binding of **P3** to Cu<sup>2+</sup>

In un-buffered water (pH 7.0), metal-free **P3** exhibits absorption bands near  $\lambda = 246$  and 279 nm, arising from the ligands HQ and Terpy, respectively. Upon addition of Cu<sup>2+</sup> ions, these two bands diminished simultaneously and new absorption bands near  $\lambda = 259$ , 317 and 330 nm appeared (Fig. 2A). Similar observations were obtained for **P3** binding with Cu<sup>2+</sup> ions in HEPES buffer (50 mM, pH 7.4): the absorption bands near  $\lambda = 250$  and 281 nm of the metal-free peptoid diminished simultaneously upon addition of Cu<sup>2+</sup> ions and new bands at  $\lambda = 260$ , 317 and 330 nm appeared (Figure S15). A metal-to-peptoid ratio plots, constructed from each titration, suggested 1:1 peptoid:Cu ratio (see inset in Fig. 2A, S14A) and the formation of the intramolecular Cu**P3** complex by simultaneous binding to both Terpy and HQ moieties.

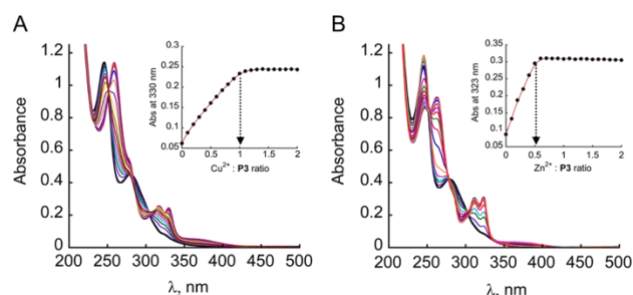


**Figure 2.** UV-Vis spectra and peptoid-to-metal ratio plot for the titration of **P3** (A) with  $\text{Cu}^{2+}$  (B) with  $\text{Zn}^{2+}$ . The peptoid (17  $\mu\text{M}$ ) in un-buffered water (pH 7.0) was titrated with 1  $\mu\text{L}$  aliquots of a metal ion (5 mM in water) in multiple steps (black = free ligand, red = metal complex). pH after the titration was not significantly altered.

To support these observations, 1 equiv. of **P3** was mixed with 1.1 equiv. of  $\text{Cu}^{2+}$  in un-buffered water (pH = 7.0), and the solution was analyzed by HR-MS techniques. The obtained mass of 1395.55 matched the calculated mass of the intramolecular 1:1  $\text{CuP3}$  complex ( $m/z = 1395.56$ , Fig. S17-18).

Next,  $\text{CuP3}$  was characterised by CD spectroscopy. In un-buffered water (pH = 7.0), the spectrum of a mixture solution containing 1 equiv. of **P3** and 1 equiv. of  $\text{Cu}^{2+}$  exhibits a double minima near 201 and 219 nm (typical for a helical Nspe peptoids, Fig. S23A,B), and an exciton couplet CD peaks between 250 and 290 nm with maximum at 257 nm and minimum at 272 nm, crossing  $\epsilon = 0$  near 260 nm. This exciton couplet is similar to the previously reported CD spectrum of  $\text{CuP1}$  complex, corresponding to the HQ  $\pi-\pi^*$  transition (Fig. S23C,D).<sup>[22b, 26]</sup> Similar observations could be seen from the CD spectrum of  $\text{CuP3}$  in HEPES buffer (10 mM, pH = 7.4); a double-minima is obtained near 204 and 221 nm, along with exciton couplet peaks corresponding to the HQ  $\pi-\pi^*$  transition appears with maximum at 256 nm and minimum at 268 nm. (Fig. S23E,F).

Finally, the binding affinity of **P3** to  $\text{Cu}^{2+}$ , was estimated by a competition experiment with EDTA.<sup>[28]</sup> Thus, a mixture of **P3** and EDTA (17  $\mu\text{M}$  each, in water, at pH = 7.0) was titrated with  $\text{Cu}^{2+}$  followed by UV-Vis spectroscopy. The obtained data was analyzed according to a previously reported method.<sup>[28b]</sup> The dissociation constant  $K_D(\text{CuP3})$ , represented by the slope between  $([\text{P3}]_{\text{total}}/[\text{CuP3}]-1)$  and  $([\text{EDTA}]_{\text{total}}/[\text{CuEDTA}]-1)$ , was found to be  $3.7 \times 10^{-16} \text{ M}$  (Figure S24). From this we calculated that the association constant  $K_A(\text{CuP3})$  is  $2.7 \times 10^{15} \text{ M}^{-1}$ .

### 2.3 Binding of **P3** to $\text{Zn}^{2+}$ and $\text{Cu}^{2+}$

Titration of metal-free **P3** with  $\text{Zn}^{2+}$  ions (up to 0.5 equiv.) in un-buffered water resulted in new absorption bands near  $\lambda = 311$  and 323 nm (Fig.2B), while almost no changes in the absorption near  $\lambda = 246$  nm was recorded (Fig. S14B), reflecting the exclusive binding of  $\text{Zn}^{2+}$  ions to the Terpy ligand. After addition of 0.5 equiv. of  $\text{Zn}^{2+}$  ions the bands at  $\lambda = 311$  and 323 nm became saturated, suggesting the formation of  $\text{Zn(P3)}_2$  (Fig. S14B). As the addition of  $\text{Zn}^{2+}$  continued, the band at  $\lambda = 246$  nm decreased and the appearance of a new band at  $\lambda = 263$  nm was recorded, indicating the binding of  $\text{Zn}^{2+}$  ions to the HQ ligands of **P3** (Fig. S14B). Metal-to-peptoid ratio plots, constructed from this titration, suggested 1:2 Zn:peptoid ratio, which is consistent with the formation of intermolecular  $\text{Zn(P3)}_2$  complex (Fig. 2B, inset) followed by the formation of the 2:2  $\text{Zn}_2(\text{P3})_2$  (Fig. S14B). ESI-MS analysis of this solution supported the formation of  $\text{Zn}_2(\text{P3})_2$  (Fig.

S19-20). In addition, ESI-MS analysis of a solution containing 1 equiv. of **P3** that was treated with 0.5 equiv. of  $\text{Zn}^{2+}$  in un-buffered water (pH = 7.0), showed a mass of 1366.60, which matched the calculated half mass of the intermolecular 1:2  $\text{Zn(P3)}_2$  complex ( $m/z = 1366.28$ , Fig. S21-22). Titration of **P3** with  $\text{Zn}^{2+}$  in HEPES buffer showed similar results (Fig. S16).

To support our observations and further characterize the formation of the intermolecular 1:2  $\text{Zn(P3)}_2$  and 2:2  $\text{Zn}_2(\text{P3})_2$  complexes, the corresponding CD spectra were recorded. To 1 equiv. of **P3**, either 0.5 equiv. or 1 equiv. of  $\text{Zn}^{2+}$  ions were added (Fig. S23G,H and I,J, respectively). Similarly to  $\text{CuP3}$ , both spectra exhibit double minima near 201, 204 and 219 nm. However, when only 0.5 equiv. of  $\text{Zn}^{2+}$  were added, the CD spectrum did not show the exciton couplet CD peaks of the HQ  $\pi-\pi^*$  transition, suggesting no binding between  $\text{Zn}^{2+}$  and the HQ ligands within **P3**. The exciton couplet CD peaks were obtained only when 1 equiv. of  $\text{Zn}^{2+}$  ions were added to **P3** (with a maximum near 269 nm and minimum at 247 nm and 278 nm, crossing at  $\epsilon = 0$  twice, near 263 nm and 279 nm), suggesting binding of  $\text{Zn}^{2+}$  to HQ ligands only when the ratio between  $\text{Zn}^{2+}$  and **P3** is 1:1. Based on these observations we can suggest the following conclusions: (i)  $\text{Zn(P3)}_2$  species, where the metal center is bound exclusively to Terpy ligands, while the HQ ligands of **P3** remain intact is formed first (up to 0.5 equiv. of  $\text{Zn}^{2+}$  per peptoid), and (ii) in the presence of 1 equiv. of  $\text{Zn}^{2+}$ , the first 0.5 equiv. of  $\text{Zn}^{2+}$  binds two Terpy ligands intermolecularly, while the additional 0.5 equiv. binds to the HQ ligands, producing 2:2 intermolecular  $\text{Zn}_2(\text{P3})_2$  species. Such a difference in  $\text{Cu}^{2+}$  versus  $\text{Zn}^{2+}$  binding to **P3** (concomitant binding to Terpy and HQ moiety for  $\text{Cu}^{2+}$  versus sequential for  $\text{Zn}^{2+}$ ) may be in line with the higher Lewis acidity of  $\text{Cu}^{2+}$  that eases the deprotonation of the HQ moiety.

As the synaptic cleft contains excess of  $\text{Cu}^{2+}$  and of  $\text{Zn}^{2+}$ , we wished to understand whether **P3** could selectively bind  $\text{Cu}^{2+}$  when both metal ions are co-present. To explore the binding of  $\text{Cu}^{2+}$  in the presence of  $\text{Zn}^{2+}$  we conducted a few experiments in HEPES buffer, where we added both  $\text{Cu}^{2+}$  and  $\text{Zn}^{2+}$  ions, as a mixed solution (the mix approach) to **P3** and characterized the formed complexes by spectroscopic techniques. As a control, we have also characterized the binding to **P3** by adding one metal after the other (the step approach). Starting with the step approach, 1 equiv. of metal-free **P3** in HEPES buffer (50 mM, pH 7.4) was treated with 0.5 equiv. of  $\text{Zn}^{2+}$  and the changes were followed by UV-Vis (Fig. 3A). The absorption band of Terpy at  $\lambda = 281$  nm diminished and two new bands appeared simultaneously near  $\lambda = 310$  and 323 nm, while the absorption band assigned to HQ showed only slight shift and no decrease in intensity, suggesting that the HQ ligands are not participating in the binding of  $\text{Zn}^{2+}$  ions, and that  $\text{Zn(P3)}_2$  is formed exclusively in line with the titration experiment. Subsequent addition of 0.5 equiv. of  $\text{Cu}^{2+}$  ions to this complex resulted in the formation of a new band at  $\lambda = 261$  nm, indicating  $\text{Cu}^{2+}$  binding to the HQ ligands and suggesting the overall formation of  $\text{ZnCu(P3)}_2$  (Fig. 3A), in which  $\text{Zn}^{2+}$  is bound to two Terpy ligands and  $\text{Cu}^{2+}$  is bound to two HQ ligands (no change in the region near 320 nm corresponding to the terpy moieties).

Continuing with a mix approach in the same reaction conditions, 1 equiv. of metal-free **P3** was treated with a mixture containing 0.5 equiv. of each  $\text{Cu}^{2+}$  and  $\text{Zn}^{2+}$ , and changes were also followed by UV-Vis. The spectrum of the obtained metallopeptoid was identical to the one obtained by the step approach (Fig. 3A), which was assigned to the formation of  $\text{ZnCu}(\text{P3})_2$ . As  $\text{Zn}^{2+}$  could bind to **P3** faster than  $\text{Cu}^{2+}$  [10a], we wanted to explore if  $\text{Cu}^{2+}$  can lead to the removal of  $\text{Zn}^{2+}$  from  $\text{Zn}_2(\text{P3})_2$ . To this aim, we have conducted an experiment in HEPES buffer, in which excess  $\text{Cu}^{2+}$  ions (1 equiv. instead of 0.5 equiv.) was added to 1 equiv. of **P3**, that was pre-incubated with 1 equiv. of  $\text{Zn}^{2+}$  to form  $\text{Zn}_2(\text{P3})_2$ . This experiment was followed by UV-Vis (Fig. 3B). The obtained spectra exhibit a gradual shift in the absorbance bands near  $\lambda = 264, 312$  and  $323$  nm, corresponding to the complex  $\text{Zn}_2(\text{P3})_2$ , until these bands fully disappear and new bands near  $\lambda = 260, 317$  and  $330$  nm appear, signifying the formation of the complex  $\text{CuP3}$  (see Fig. 2A above). At the working concentration of  $20 \mu\text{M}$ , the metal exchange has a  $t_{1/2}$  of about 170s. The Cu, Zn complexes formation with **P3** was also probed by Electronic-Paramagnetic-Resonance (EPR, Fig. S26). Under our sample preparation conditions ( $>10$  min), we detect only the  $\text{CuP3}$  complex regardless of the presence of Zn. Overall, our results suggest that upon mixing molar equiv. of **P3**,  $\text{Cu}^{2+}$  and  $\text{Zn}^{2+}$  ions in HEPES buffer, the complexes  $\text{ZnCu}(\text{P3})_2$  (not detected in the time scale of EPR sample preparation), and/or  $\text{Zn}_2(\text{P3})_2$ , are formed first as kinetic products, and these will react selectively with the remaining  $\text{Cu}^{2+}$  to form  $\text{CuP3}$  as a single thermodynamic product (Fig. 3C). This conclusion indicated that **P3** is indeed selective to  $\text{Cu}^{2+}$  in the relevant conditions and concentrations, encouraging us to further explore the ability of **P3** to remove  $\text{Cu}^{2+}$  from  $\text{A}\beta$  and inhibit the production of ROS.

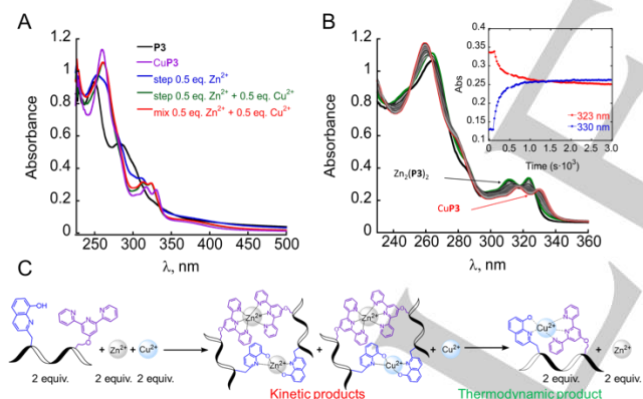


**Figure 3.** (A) UV-Vis spectra describing  $\text{Cu}^{2+}$  binding to **P3** in the presence of  $\text{Zn}^{2+}$ . (B) UV-Vis titration of  $\text{Zn}(\text{P3})_2$  complex with excess of  $\text{Cu}^{2+}$ . Inset: Kinetics of decrease in absorbance of  $\text{Zn}(\text{P3})_2$  ( $323$  nm) and simultaneous increase in the absorbance of  $\text{CuP3}$  ( $330$  nm). Conditions:  $20 \mu\text{M}$  of peptoid or peptoid complex in HEPES buffer ( $50$  mM,  $\text{pH}$  7.4) treated with 0.5 or 1 equiv. of  $\text{Cu}^{2+}$ . (C) A schematic representation of complexes formation from 2 equiv. of **P3**, 2 equiv.  $\text{Cu}^{2+}$  and 2 equiv.  $\text{Zn}^{2+}$  using the mix approach, showing the formation of kinetic and thermodynamic products.

## 2.4 Reactive oxygen species production

To probe ROS production, two approaches could be used. The first approach includes following the consumption of ascorbate by UV/Vis at  $265$  nm ( $\epsilon = 14\,500 \text{ M}^{-1}\text{cm}^{-1}$ ), the reductant that fuels the formation of  $\text{H}_2\text{O}_2$  or  $\text{HO}^\cdot$ . [29] In the second approach, the formation of  $\text{HO}^\cdot$  is followed by monitoring the fluorescence intensity of 7-hydroxy-coumarin-3-carboxylic acid (7-OH-CCA)

dye that forms as a result of the reaction between  $\text{HO}^\cdot$  with coumarin-3-carboxylic acid (CCA). [30] The metal-ion binding sites of  $\text{A}\beta$  to Cu and Zn lie within residues 1-16, [31] therefore we have focused our study on the monomeric peptide  $\text{A}\beta_{1-16}$  complex. In addition to it, the fibrillary forms of  $\text{A}\beta$  showed less activity than the monomeric peptide by one order of magnitude, [32] making the  $\text{A}\beta_{1-16}$  peptide a good model for investigation.

Starting with the first approach, it was previously shown that, while a rapid consumption of ascorbate takes place in the presence of unbound copper, regardless of the co-presence of  $\text{Zn}^{2+}$  in the tested medium, when copper is bound to  $\text{A}\beta$ , this consumption slows down. [10, 11a, 29, 32, 33] We therefore conducted ascorbate consumption experiments in order to evaluate the effect of **P3** on the production of ROS by Cu (in blue) or  $\text{Cu-A}\beta$  (in red) in the absence (Fig. 4, A-C) and in the presence (Fig. 4, D-F) of  $\text{Zn}^{2+}$ . In order to simulate all possible conditions for probing ROS production, three different ascorbate consumption experiments with three different starting points were performed: (1) starting from  $\text{Cu}^{2+}$  (Fig. 4A, D) (2) starting from  $\text{Cu}^+$  (Fig. 4B, E) and (3) starting from a mixture of  $\text{Cu}^+$  and  $\text{Cu}^{2+}$  (Fig. 4C, F). In the first experiment, **P3** was added to  $\text{Cu}^{2+}$  or  $\text{Cu}^{2+}\text{-A}\beta$  under aerobic conditions, followed by the addition of ascorbate. In the second experiment,  $\text{Cu}^+$  or  $\text{Cu}^+\text{-A}\beta$  are generated in situ by mixing these together with ascorbate under anaerobic conditions, followed by the addition of **P3** and then the sample was exposed to air to trigger the ascorbate consumption. In the last experiment, ascorbate was added to  $\text{Cu}^{2+}$  or  $\text{Cu}^{2+}\text{-A}\beta$  under aerobic conditions, followed by the addition of **P3**. Notably, in the third experiment, **P3** was added when the intensity was decreased from about 1.8 to about 0.9-1. As seen in Fig. 4, each addition led to an increase in the intensity of the absorbance at  $265$  nm, which is attributed to the formation of the metal-peptoid complex (UV-Vis spectra of Cu and Zn complexes with **P3** are shown in Fig. S25). After the addition of the last component, when the catalytic cycle should start, either no change in the intensity of the absorbance at  $265$  nm was observed, indicating no ascorbate consumption and thus no ROS production, or a sharp intensity decrease occurred, which suggests the consumption of ascorbate and formation of ROS.

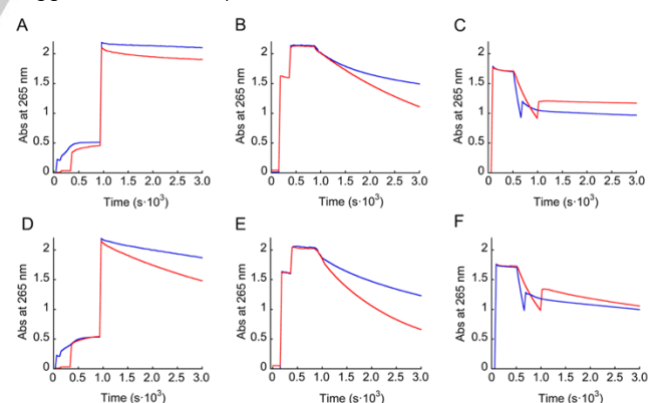


**Figure 4.** Kinetics of ascorbate consumption, followed by UV/vis at  $265$  nm. (A)  $\text{Cu}^{2+} + \text{P3} + \text{Asc}$  (blue),  $\text{A}\beta_{1-16} + \text{Cu}^{2+} + \text{P3} + \text{Asc}$  (red). (B)  $\text{Cu}^{2+} + \text{Asc} + \text{P3} + \text{air}$  (blue),  $\text{A}\beta_{1-16} + \text{Cu}^{2+} + \text{Asc} + \text{P3} + \text{air}$  (red). (C)  $\text{Asc} + \text{Cu}^{2+} + \text{P3}$  (blue),  $\text{Asc} + \text{A}\beta_{1-16} + \text{Cu}^{2+} + \text{P3}$  (red). (D)  $\text{Cu}^{2+} + \text{Zn}^{2+} + \text{P3} + \text{Asc}$  (blue),  $\text{A}\beta_{1-16} + \text{Cu}^{2+} + \text{Zn}^{2+} + \text{P3} + \text{Asc}$  (red). (E)  $\text{Cu}^{2+} + \text{Zn}^{2+} + \text{Asc} + \text{P3} + \text{air}$  (blue),  $\text{A}\beta_{1-16} + \text{Cu}^{2+} + \text{Zn}^{2+} + \text{Asc} + \text{P3} + \text{air}$  (red). (F)  $\text{Asc} + \text{Cu}^{2+} + \text{Zn}^{2+} + \text{P3}$  (blue),  $\text{Asc} + \text{A}\beta_{1-16} + \text{Cu}^{2+} + \text{Zn}^{2+} + \text{P3}$  (red). The order of components in the text (A-F) represents the order of addition of the components in the cuvette. Conditions:  $[\text{P3}] = [\text{A}\beta_{1-16}] = [\text{Zn}^{2+}] = 10 \mu\text{M}$ ,  $[\text{Cu}^{2+}] = 9 \mu\text{M}$ ,  $[\text{Asc}] = 100 \mu\text{M}$ ,  $[\text{HEPES}] = 50$  mM,  $\text{pH} = 7.4$ , with background subtraction of the signal at  $800$  nm.

## RESEARCH ARTICLE

Looking at Fig. 4A-C, we can see that **P3** is able to stop ascorbate consumption by both free Cu and Cu-A $\beta$  complex only in experiments (1) and (3), while in experiment (2), when Cu<sup>2+</sup> is added together with ascorbate in anaerobic conditions to form Cu<sup>+</sup>, **P3** can only slow down the ascorbate consumption but not stop it (Fig. 4B), indicating that **P3** doesn't bind Cu<sup>+</sup> under a redox inert form and/or can not extract Cu<sup>+</sup> from Cu-A $\beta$  complex. Interestingly, when **P3** was added in the presence of Zn<sup>2+</sup> in all three experiments, the ascorbate consumption did not stop immediately but rather, only slowed down (Fig. 4D&F). These results indicate that the presence of Zn<sup>2+</sup> ions limit the extraction of Cu<sup>2+</sup> from Cu<sup>2+</sup>-A $\beta$  complex by **P3**. As a control, the same experiments in the same conditions were done in the absence of **P3** (Fig. S33A-F), showing full ascorbate consumption.

Our conclusions from the UV-Vis experiments were further examined by measurements performed according to the second approach, in which the formation of HO $\cdot$  in the same experimental setups was followed by monitoring the fluorescence intensity of CCA. The results obtained from these fluorescence assays (Fig. S34) matched perfectly those obtained from the ascorbic consumption experiments, supporting the ability of **P3** to prevent the ROS production caused by either free Cu ions or Cu-A $\beta$ .

The limited ability of **P3** to stop the ROS production in the presence of Zn<sup>2+</sup> ions is explained by our observation that Zn(**P3**)<sub>2</sub>, ZnCu(**P3**)<sub>2</sub> complexes are formed first as the kinetic products, while the Cu**P3** is formed slower, as the thermodynamic product. Thus, **P3** should first bind mainly Zn<sup>2+</sup>, leaving Cu-A $\beta$  mostly intact, thus leading to ROS production, followed by the extraction of Cu<sup>2+</sup> by **P3** complexes, eventually resulting in the arrest of ROS production. It should be noted that the formation of the A $\beta$ -Cu/Zn-**P3** ternary species, where Cu remains partially bound to A $\beta$ , and therefore continues to participate in the redox cycle, could occur in parallel to described above events. Formation of ternary species has been reported to occur at physiological conditions [3a,b, 34], and therefore should be excluded from the possible pathway of action of **P3**, and full extraction of Cu from Cu/CuZn-A $\beta$  complex should be proven first. To support full extraction of Cu from CuA $\beta$ /CuZnA $\beta$  complex by **P3**, CD and EPR experiments were performed.

### 2.5 Cu<sup>2+</sup> extraction from Cu-A $\beta$ complex in the absence and presence of Zn<sup>2+</sup>

After having shown the thermodynamic selectivity of **P3** for Cu<sup>2+</sup> (compared to Zn<sup>2+</sup>) and the likely Zn<sup>2+</sup>-induced slow-down of ROS lessening by **P3**, we investigated by CD and EPR whether **P3** has a higher selectivity than A $\beta$ , a pre-requisite to remove Cu<sup>2+</sup> from A $\beta$  in presence of Zn<sup>2+</sup> [3a, 10]. The CD spectrum of free A $\beta$ <sub>1-16</sub> in HEPES buffer (10 mM, pH = 7.4) exhibits two bands with a minimum near 201 nm and a maximum near 223 nm (Fig. S36A), indicating the presence of the polyproline type II (PPII) helical structure conformation, as previously reported.<sup>[35]</sup> The addition of 1 equiv. of Cu<sup>2+</sup> to the solution resulted in an intensity decrease of both bands, indicating the weakening of the helical conformation of A $\beta$ <sub>1-16</sub> resulted from the partial change of it to  $\beta$ -sheet upon binding to Cu<sup>2+</sup> ions [35]. In contrast, addition of 1 equiv. of Zn<sup>2+</sup> to 1 equiv. of A $\beta$ <sub>1-16</sub> showed a slight increase in the positive band near 223 nm (Fig. S36B-C), suggesting that ZnA $\beta$  species maintain the initial conformational preference, and that the Zn<sup>2+</sup> ions rather stabilize the overall conformation of A $\beta$ <sub>1-16</sub> at the chosen conditions. Interestingly, when both Cu<sup>2+</sup> and Zn<sup>2+</sup> were added to a solution of 1 equiv. of A $\beta$ <sub>1-16</sub>, the obtained spectrum

resembled the spectrum of CuA $\beta$ , suggesting that Cu<sup>2+</sup> binds to the same binding site in both experiments and that Zn<sup>2+</sup> ions do not interfere strongly with the binding to A $\beta$ <sub>1-16</sub>, in line with previous report.<sup>[29]</sup> The changes in the positive band of A $\beta$ <sub>1-16</sub> upon its binding to the metal ions are summarized in Fig. S36.

As the addition of Cu<sup>2+</sup> to A $\beta$ <sub>1-16</sub> leads to a decrease in the absorbance band near 200 nm, extraction of Cu<sup>2+</sup> by **P3** should lead to an increase in intensity of this band. However, **P3** has an intense minimum near 200 nm, thus it is difficult to make a conclusion reading the extraction of Cu<sup>2+</sup> based on this band. In contrast, **P3**, Zn(**P3**)<sub>2</sub>, A $\beta$ <sub>1-16</sub>, CuA $\beta$ , ZnA $\beta$  and CuZnA $\beta$  do not absorb at the 250-300 nm range (see SI), while Cu**P3** and Zn<sub>2</sub>(**P3**)<sub>2</sub> exhibit band(s) in this range with a minimum near 270 nm (Cu**P3**, Fig. 5A and S23D,F) or with a maximum near 270 nm and a minimum near 280 nm (Zn<sub>2</sub>(**P3**)<sub>2</sub>, Fig. 5B and 23J). Therefore, obtaining a single minimum band near 270 nm in competition experiments between A $\beta$ <sub>1-16</sub> and **P3** for Cu<sup>2+</sup> binding will be a clear indication for the exclusive formation of Cu**P3**.

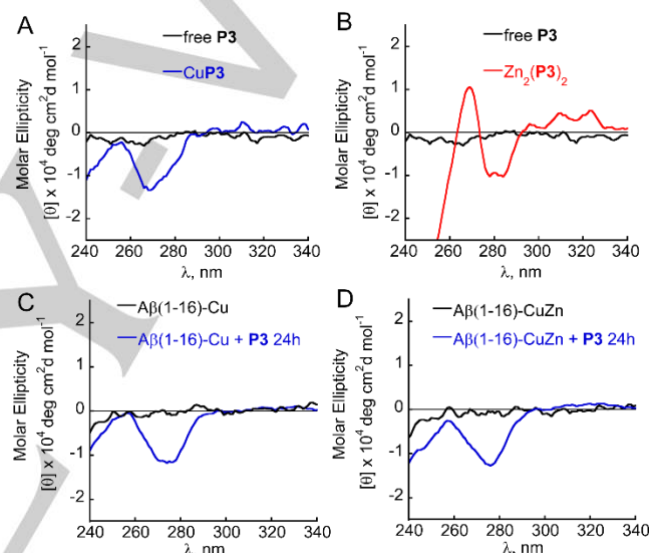


**Figure 5.** CD studies for Cu<sup>2+</sup> extraction from Cu-A $\beta$  complex in the absence and presence of Zn<sup>2+</sup>. CD spectrum of the near UV range for (A) free **P3** (black) and Cu<sup>2+</sup> + **P3** (blue) (B) free **P3** (black) and Zn<sup>2+</sup> + **P3** (red) (C) A $\beta$ <sub>1-16</sub> + Cu<sup>2+</sup> (black) and A $\beta$ <sub>1-16</sub> + Cu<sup>2+</sup> + **P3** (blue) (D) A $\beta$ <sub>1-16</sub> + Cu<sup>2+</sup> + Zn<sup>2+</sup> (black) and A $\beta$ <sub>1-16</sub> + Cu<sup>2+</sup> + Zn<sup>2+</sup> + **P3** (blue). The order of components in the cuvette. Conditions: [**P3**] = [A $\beta$ <sub>1-16</sub>] = [Zn<sup>2+</sup>] = 100  $\mu$ M, [Cu<sup>2+</sup>] = 90  $\mu$ M, [HEPES] = 10 mM, pH=7.4.

To probe this point, extraction of Cu from CuA $\beta$  complex by **P3** in the absence and presence of Zn was studied by CD spectroscopy. First, mixtures of 1 equiv. of A $\beta$ <sub>1-16</sub> and Cu<sup>2+</sup> or Cu<sup>2+</sup>/Zn<sup>2+</sup> mixture (0.9 equiv. and 0.9:1 equiv., respectively) in HEPES buffer (10 mM, pH = 7.4) were allowed to react for 5 min and then their CD spectra were recorded and compared to the CD of **P3** in the same conditions (Fig. 5C,D, black curves). Next, 1 equiv. of **P3** were added to the mixtures and the solutions were incubated for 24 hours, before their CD spectra were measured and compared to the spectrum of **P3** with Cu<sup>2+</sup> (Fig. 5C,D blue curves, and S37). These spectra show a single band with a minimum between 270-280 nm, resembling the spectrum of Cu**P3**, which suggest the successful extraction of Cu from CuA $\beta$ /CuZnA $\beta$  complex.

To further probe the ability of **P3** to remove Cu<sup>2+</sup> from A $\beta$ <sub>1-16</sub>, EPR is the method of choice.<sup>[10a]</sup> Figure 6 shows the monitoring of A $\beta$ <sub>1-16</sub>-bound Cu<sup>2+</sup> extraction by **P3** in absence of Zn, with the

## RESEARCH ARTICLE

sample frozen as soon as possible after addition of **P3** (panel A, red line) and after 2 hours (panel A, blue line). In panel B, the same experiment is performed on CuZnA $\beta$  complex. In green lines, are the EPR signature of Cu-**P3**, in black lines that of Cu<sup>2+</sup>-A $\beta$ <sub>1-16</sub> or CuZnA $\beta$  in presence of one equiv. of Zn and in red and blue lines the resulting species after addition of **P3**. Cu-**P3** is characterized by the following <sup>65</sup>Cu-EPR parameters:  $g_{\parallel} = 2.26$ ,  $A_{\parallel} = 160 \cdot 10^{-4} \text{ cm}^{-1}$  and  $g_{\perp} = 2.06$ , while the signature of Cu-A $\beta$ <sub>1-16</sub> is identical as that previously reported with two species co-existing at pH 7.4<sup>[31, 36]</sup>. Hyperfine lines of Cu-**P3** and Cu-A $\beta$ <sub>1-16</sub> are shown in plain and dotted lines, respectively. In absence of Zn, and upon addition of **P3**, the EPR signature corresponds to a mixture of Cu-A $\beta$ <sub>1-16</sub> and Cu-**P3** species in about a 1:1 ratio (panel A, red line). After two hours (panel A, blue line), the EPR signature of the mixture is superimposable to that of Cu-**P3**. In presence of Zn, the spectrum recorded immediately after **P3** addition is similar to the one of Cu-A $\beta$  (panel B, red line) while after two hours, the signature of Cu-**P3** is detected (panel B, blue line). The EPR experiment perfectly demonstrates that (i) Cu is removed from A $\beta$ <sub>1-16</sub> regardless of the presence of Zn and (ii) in presence of Zn, the Cu extraction takes more time. In other words, the thermodynamic Cu over Zn selectivity of **P3** is fully appropriate,<sup>[10b, 3b]</sup> while Zn has a kinetic effect on the Cu<sup>2+</sup> extraction from A $\beta$ <sub>1-16</sub>.

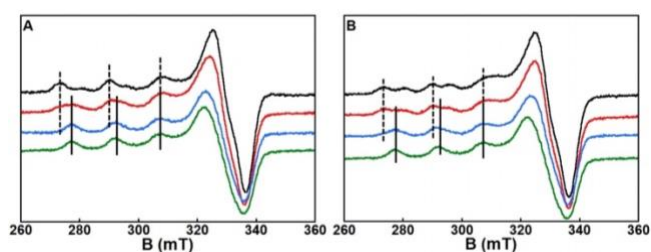


**Figure 6.** EPR spectra of (A) Cu<sup>2+</sup> + **P3** (green), A $\beta$ <sub>1-16</sub> + Cu<sup>2+</sup> (black), A $\beta$ <sub>1-16</sub> + Cu<sup>2+</sup> + **P3** - EPR tube frozen asap (red) and A $\beta$ <sub>1-16</sub> + Cu<sup>2+</sup> + **P3** - EPR tube frozen after two hours (blue). (B) Cu<sup>2+</sup> + **P3** (green), A $\beta$ <sub>1-16</sub> + Cu<sup>2+</sup> + Zn<sup>2+</sup> (black)<sup>[a]</sup>, A $\beta$ <sub>1-16</sub> + Cu<sup>2+</sup> + Zn<sup>2+</sup> + **P3** - EPR tube frozen asap (red), A $\beta$ <sub>1-16</sub> + Cu<sup>2+</sup> + Zn<sup>2+</sup> + **P3** - EPR tube frozen after two hours (blue). [a] note that the difference in the EPR signature of Cu- A $\beta$ <sub>1-16</sub> with or without Zn is due to the co-binding of Zn to the Ab peptide and has been documented before.<sup>[29]</sup> Conditions: [**P3**] = [A $\beta$ <sub>1-16</sub>] = [Zn<sup>2+</sup>] = 200  $\mu\text{M}$ , [Cu<sup>2+</sup>] = 180  $\mu\text{M}$ , [HEPES] = 50 mM, pH=7.4. Recording conditions: T = 120 K,  $\nu$  = 9.5 GHz, modulation amplitude = 5 G, microwave power: 20 mW.

Overall, the CD and EPR experiments exclude the possible formation of A $\beta$ -Cu/Zn-**P3** ternary species in significant amount. To further explore whether the limited ability of **P3** for immediate arrest of ROS production in the presence of Zn<sup>2+</sup> is indeed related to the differences in kinetics of Cu<sup>2+</sup> and Zn<sup>2+</sup> coordination to **P3**, we set to evaluate the rates of Cu<sup>2+</sup> and Zn<sup>2+</sup> binding to **P3** in the relevant reaction conditions.

## 2.6 Kinetic study

To evaluate to which of the metal ions, Cu<sup>2+</sup> or Zn<sup>2+</sup>, **P3** coordinates first, we measured the rates of Cu<sup>2+</sup> and Zn<sup>2+</sup> binding to **P3** in the presence of A $\beta$  peptide. Thus, 1 equiv. of **P3** was added to a buffered solution of quasi-stoichiometric amount of each metal ion (0.9 equiv. of Cu<sup>2+</sup> and/or 1 equiv. of Zn<sup>2+</sup>, respectively) and 1 equiv. of A $\beta$ , and followed by addition of 1 equiv. of **P3**. The A $\beta$  and metal ions were allowed to react for 500 s to ensure complex formation prior to the addition of 1 equiv. of **P3**. The reactions were followed by UV-Vis spectroscopy and the

results are depicted in Fig. 7A-D. In the case of single metal-peptoid complex formation, we can see that while Cu<sup>2+</sup> binds faster than Zn<sup>2+</sup> to the HQ binding site of **P3** (Fig. 7A, green versus black, respectively (formation of complex); and purple versus blue, respectively (consumption of **P3**), both Cu<sup>2+</sup> and Zn<sup>2+</sup> bind at similar rate to the Terpy site (Fig. 7B, blue and red curves, respectively). In the presence of the mixture of both Cu<sup>2+</sup> and Zn<sup>2+</sup> metal ions plots several observations could be made: (i) the reactions are faster as expected due to double concentration of the metal ions; (ii) the decrease in the curves showed in Fig. 7D indicates that the Terpy binding site of **P3** initially binds Zn<sup>2+</sup>, followed by binding of Cu<sup>2+</sup> (see also Fig. S40, where the arrow indicates a shift of metal-complex absorption band from 311-323 nm for Zn**P3** species towards 317-330 nm, that corresponds to Cu**P3** species); (iii) the slight decrease in the curves showed in Fig. 7C (green and black curves) can suggest the simultaneous formation of several species; the overall decrease (Fig. 7C) indicates that like the Terpy site, the HQ site of **P3** initially binds Zn<sup>2+</sup>, followed by the binding of Cu<sup>2+</sup> (see also Fig. S40, where the arrow in spectra indicates shift of metal-complex absorption band from 264 nm for Zn**P3** species towards 260 nm, that corresponds to Cu**P3** species).

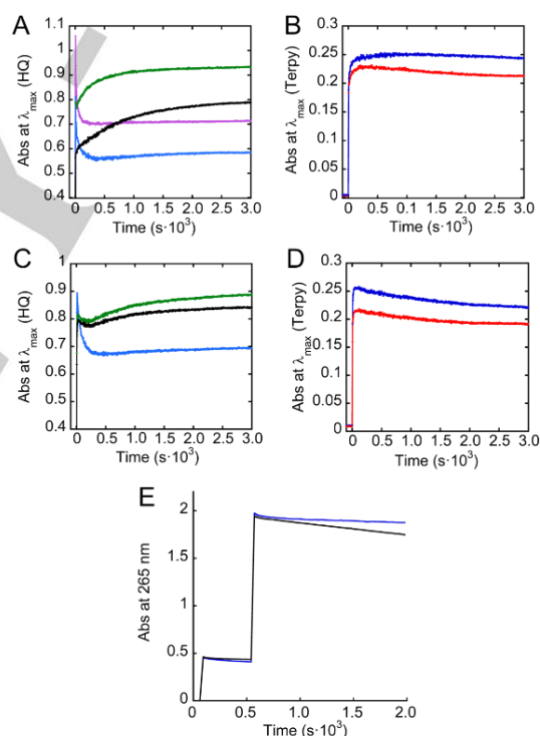
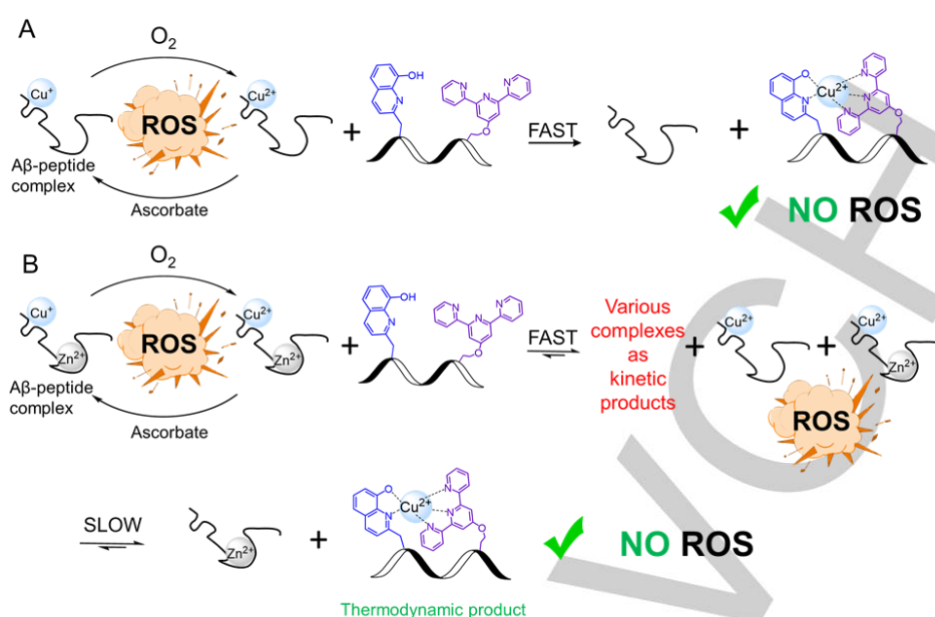


**Figure 7.** Kinetics of Cu or Zn extraction by **P3** from CuA $\beta$  or ZnA $\beta$  at (A) HQ region: Cu<sup>2+</sup>A $\beta$ <sub>1-16</sub> + **P3** at 250 nm (purple) and at 260 nm (green), and Zn<sup>2+</sup>A $\beta$ <sub>1-16</sub> + **P3** at 250 nm (light blue) and at 264 nm (black); (B) Terpy region: Cu<sup>2+</sup>A $\beta$ <sub>1-16</sub> + **P3** at 329 nm (blue) and Zn<sup>2+</sup>A $\beta$ <sub>1-16</sub> + **P3** at 323 nm (red). Kinetics of Cu,Zn competition extraction by **P3** from the Cu,Zn-A $\beta$  complex at (C) HQ region: Cu<sup>2+</sup>,Zn<sup>2+</sup>-A $\beta$ <sub>1-16</sub> + **P3** at 250 nm (light blue), at 260 nm (green) and at 264 nm (black) or (D) Terpy region: Cu<sup>2+</sup>,Zn<sup>2+</sup>-A $\beta$ <sub>1-16</sub> + **P3** at 329 nm (blue) or at 323 nm (red) Conditions: [**P3**] = [A $\beta$ <sub>1-16</sub>] = [Zn<sup>2+</sup>] = 20  $\mu\text{M}$ , [Cu<sup>2+</sup>] = 18  $\mu\text{M}$ , [HEPES] = 50 mM, pH=7.4, with background subtraction of the signal at 800 nm. Additions of **P3** were performed at t = 0s. (E) Ascorbate consumption in pre-incubated solution of Cu<sup>2+</sup>A $\beta$ <sub>1-16</sub>-**P3** (blue curve) or Cu<sup>2+</sup>Zn<sup>2+</sup>-A $\beta$ <sub>1-16</sub>-**P3** (black curve) for 24 hours. Ascorbate was added at t = 541s to ensure that the absorbance intensity of the formed species is stabilized. Conditions: [**P3**] = [A $\beta$ <sub>1-16</sub>] = [Zn<sup>2+</sup>] = 10  $\mu\text{M}$ , [Cu<sup>2+</sup>] = 9  $\mu\text{M}$ , [Asc] = 100  $\mu\text{M}$ , [HEPES] = 50 mM, pH 7.4, with background subtraction of the signal at 800 nm.



**Scheme 2.** Schematic summary of Cu chelation and ROS production/inhibition by the peptoid **P3** in the presence of ascorbate and A $\beta$  and in the absence (A) or presence (B) of Zn<sup>2+</sup>.

Overall, the kinetic data demonstrates that in the presence of Zn<sup>2+</sup> the extraction of Cu<sup>2+</sup> ions by **P3** is slowed down by the formation of Zn**P3** complexes as kinetic products, and this hinders the immediate inhibition of ROS production. However, our data shows that **P3** can extract Cu<sup>2+</sup> ions in the presence of Zn<sup>2+</sup>, which leads to the formation of Cu**P3** as the thermodynamic product and results in some inhibition of ROS production also in the presence of Zn<sup>2+</sup>. As the full extraction of Cu<sup>2+</sup> by **P3** is a thermodynamic process, we wanted to see if we could increase ROS inhibition using this result. To this aim, Cu<sup>2+</sup> and Zn<sup>2+</sup> ions were added simultaneously to A $\beta$  to form the complexes Cu-A $\beta$  or CuZn-A $\beta$ , (as indicated by UV-Vis, Fig. S41A), followed by the addition of **P3**, and the solution was incubated for 24 hours. After 24 hours, the UV-Vis spectrum of this solution was measured (Fig. S41B), and the obtained spectrum in the presence of Zn<sup>2+</sup> indicated the formation of the mixture of species. Thereafter ascorbate was added, and the spectrum showed almost no consumption - 12 % consumption (Fig. 7E) vs. 32 % consumption in 25 min for the same experiment, performed without pre-incubation (Fig. 4D). These results, together with the data presented in Fig. 4D-F, support the extraction Cu<sup>2+</sup> from CuZn-A $\beta$  by **P3** to form Cu**P3** via a thermodynamic process, and allow for almost full inhibition of ROS production also in the presence of Zn<sup>2+</sup> ions.

To correlate the amount of **P3**-bound Cu<sup>2+</sup> and Zn<sup>2+</sup> with the amount of ascorbate that is consumed during the reaction, we constructed a calibration curve by following the addition of 1 equiv. of **P3** to a set of Cu<sup>2+</sup> and Zn<sup>2+</sup> mixtures in different equiv. ratios, via UV-Vis (Fig. S42). The recorded spectrum of each mixture was compared to the corresponding spectrum obtained from the ascorbate consumption experiments. The results (Table S5-6 and Fig. S43) suggest the following: (i) without pre-incubation, about 50-70 % of Cu<sup>2+</sup> and 30-50 % of Zn<sup>2+</sup> are bound to the **P3**, which is in agreement with the amount of ascorbate consumption (about 32 %), (ii) with pre-incubation, about 80-90 % of Cu<sup>2+</sup> and no more than 10-20 % of Zn<sup>2+</sup> are bound to the **P3**, and this also correlates

with the amount of ascorbate consumption in this case (about 12 %).

Our observations support our hypothesis as depicted in Scheme 2: in the absence of Zn<sup>2+</sup>, the extraction of Cu<sup>2+</sup> from A $\beta$  is immediate, and so is ROS inhibition, which is fully achieved (scheme 2A), while in the presence of Zn<sup>2+</sup> the extraction of Cu<sup>2+</sup> ions by **P3** is slower than the extraction of Zn<sup>2+</sup> and therefore various complexes are formed as kinetic products, hindering the immediate inhibition of ROS production (scheme 2B).

## Conclusions

Herein we showed that the incorporation of one piperazine group at the C-terminus of a water-insoluble hydrophobic helical peptoid chelator with high selectivity to Cu<sup>2+</sup> resulted in the water-soluble peptoid chelator **P3**. We demonstrated that the selectivity of **P3** to Cu<sup>2+</sup>, in the presence of excess of other metal ions, including Zn, is preserved also in water. Selectivity to Cu in the presence of Zn is extremely important in the context of AD, because the ionic pool of the synaptic cleft, where A $\beta$  aggregation and ROS production take place, contains excess of Zn, which can potentially hinder Cu binding by an external chelator due to possible similarities in the binding preferences of these two metal ions. However, we show that **P3** binds Cu<sup>2+</sup> and Zn<sup>2+</sup> differently: Cu<sup>2+</sup> binds HQ and Terpy simultaneously, leading exclusively to the 1:1 metal:peptoid intramolecular Cu**P3** complex, while Zn<sup>2+</sup> binds first two Terpy ligands from two peptoids in a 1:2 metal:peptoid ratio, forming the intermolecular Zn(**P3**)<sub>2</sub> complex, followed by the binding of additional equiv. of Zn or Cu<sup>2+</sup> that are present in solution, forming the complexes Zn<sub>2</sub>(**P3**)<sub>2</sub> or ZnCu(**P3**)<sub>2</sub>, respectively.

Despite the fast formation of Zn complexes being kinetically favored products, as illustrated from the mixture and step approach and kinetic studies, Cu<sup>2+</sup> ions can replace Zn from these complexes, resulting in the formation of Cu**P3** as an exclusive



thermodynamic product. Furthermore, we show here for the first time, that the selectivity of this water-soluble peptoid chelator, **P3**, to  $\text{Cu}^{2+}$  can be used in the context of AD: **P3** can successfully extract  $\text{Cu}^{2+}$  from the  $\text{CuA}\beta$ -complex even in the presence of Zn ions, to form the thermodynamically stable complex  $\text{CuP3}$ , and by this enables the inhibition of ROS production in a reducing environment at physiological pH (Scheme 2), as confirmed by both ascorbate consumption experiments and CCA Fluorescence assays. These unique abilities of **P3**, combined with the advantages of peptoids as therapeutics including their high proteolytic resistance, high membrane permeability and tolerance towards high salts concentrations, make **P3** an excellent chelator compared to the other peptidomimetic ligands known as drug candidates in a context of AD.

Further studies will focus on possible modifications of the **P3** sequence to allow full arrest of ROS production caused by  $\text{CuA}\beta$ -complex, in physiological conditions and in biological systems. In addition, the effect of **P3**, as well as similar peptoid chelators, on the aggregation of  $\text{A}\beta$  peptides, associated with high toxicity, will be further evaluated.

## Acknowledgements

This work was supported by the Israel Science Foundation (ISF) grant number 395/16 awarded to G. M. and by the European Council of Science (ERC) grant StG638712 "aLzINK" awarded to C. H. The authors thank Mrs. Larisa Panz for her assistance with MS measurements. A. B. thanks the Schulich Foundation for her PhD fellowship.

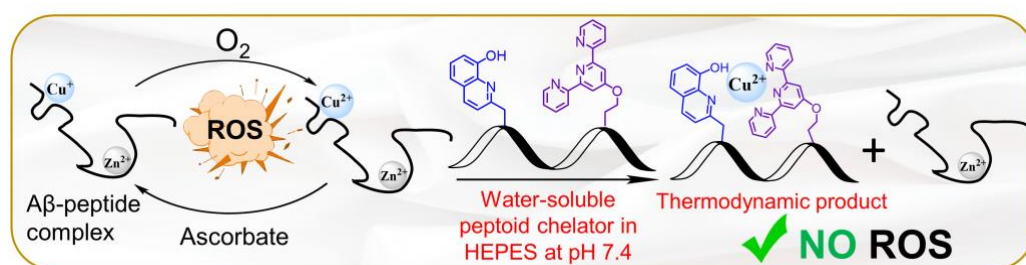
## Conflicts of interest

There are no conflicts to declare.

**Keywords:** peptoid • peptide • Cu chelator • Alzheimer disease • Zn • amyloid

## Entry for the Table of Contents

## RESEARCH ARTICLE



Cu-chelation from Amyloid- $\beta$  ( $A\beta$ ) peptide complex is a known approach towards the development of therapeutics for Alzheimer's Disease (AD), the most common form of dementia. Herein we describe a water-soluble peptidomimetic chelator that removes Cu from Cu- $A\beta$  in the presence of Zn, forming the thermodynamically stable Cu-chelator complex, and by this enables the inhibition of ROS production in a reducing environment at physiological pH.

- [1] E. I. Solomon, D. E. Heppner, E. M. Johnston, J. W. Ginsbach, J. Cirera, M. Qayyum, M. T. Kieber-Emmons, C. H. Kjaergaard, R. G. Hadt, L. Tian, *Chem. Rev.*, **2014**, *114* (7), 3659-3853.
- [2] A. I. Bush, *Curr. Opin. Chem. Biol.*, **2000**, *4*, 184.
- [3] (a) M. G. Savelieff, G. Nam, J. Kang, H. J. Lee, M. Lee, and Mi Hee Lim, *Chem. Rev.*, **2019**, *119* (2), 1221-1322; (b) C. Esmieu, D. Guettas, A. Conte-daban, L. Sabater, P. Faller and C. Hureau, *Inorg. Chem.*, **2019**, *58* (20), 13509-13527; (c) C. Cheignon, M. Tomas, D. Bonnefont-Rousselot, P. Faller, C. Hureau, F. Collin, *Redox Biol.*, **2018**, *14*, 450-464; (d) E. Atrián-Blasco, P. Gonzalez, A. Santoro, B. Alies, P. Faller and C. Hureau, *Coord. Chem. Rev.*, **2018**, *375*, 38-55.
- [4] (a) P. Faller, C. Hureau, and O. Berthoumieu, *Inorg. Chem.*, **2013**, *52*(21), 12193-12206; (b) A. Tiiman, P. Palumaa and V. Tõugu, *Neurochem. Int.*, **2013**, *62*, 367-378.
- [5] (a) S. Ayton, P. Lei and A.I. Bush, *Neurotherapeutics*, **2015**, *12*, 109-120; (b) V. Chiurchiù, A. Orlacchio, M. Maccarrone, *Oxid Med Cell Longev.* **2016**, *2016*, 7909380; (c) N. Xia, L. Liu, *Mini-Rev. Med. Chem.*, **2014**, *14*(3), 271-281; (d) P. J. Crouch and K. J. Barnham, *Acc. Chem. Res.*, **2012**, *45*(9), 1604-1611; (e) K. J. Barnham, A. I. Bush, *Chem. Soc. Rev.*, **2014**, *43*, 6727-6749; (f) A. Robert, Y. Liu, M. Nguyen and B. Meunier, *Acc. Chem. Res.*, **2015**, *48* (5), 1332-1339; (g) C. Hureau and P. Faller., *Biochimie*, **2009**, *91* (10), 1212-1217.
- [6] (a) J. Kardos, I. Kovfics, F. Hajs, M. Kfilmfin, and M. Simonyi, *Neurosci. Lett.*, **1989**, *103*, 139-144; (b) D. E. Hartter and A. Barnea, *Synapse*, **1988**, *2*, 412-415; (c) C. J. Frederickson, *Int. Rev. Neurobiol.*, **1989**, *31*, 145-238.
- [7] (a) I. Zawisa, M. Rozga and W. Bal, *Coord. Chem. Rev.*, **2012**, *256* (19-20), 2297-2307; (b) S. Noël, S. Bustos, S. Sayen, E. Guillon, P. Faller and C. Hureau, *Metalomics*, **2014**, *6*, 1220-1222.
- [8] B. Alies, E. Renaglia, M. Rozga, W. Bal, P. Faller and Hureau C., *Anal. Chem.*, **2013**, *85* (3), 1501-1508.
- [9] C. Hureau in *Encyclopedia of Inorganic and Bioinorganic Chemistry*, (eds: R.A. Scott), John Wiley & Sons Ltd, **2018**, pp. 1-14.
- [10] (a) A. Conte-Daban, A. Day, P. Faller and C. Hureau, *Dalton Trans.*, **2016**, *45*, 15671-15678; (b) E. Atrian-Blasco, A. Conte-Daban and C. Hureau, *Dalton Trans.*, **2017**, *46*, 12750-12759.
- [11] (a) P. Faller and C. Hureau, *Dalton Trans.*, **2009**, 1080-1094; (b) M. A. Santos, K. Chand and S. Chaves, *Coord. Chem. Rev.*, **2016**, *327-328*, 287-303.
- [12] S.C. Drew, *Front. Neurosci.*, **2017**, *11*, 317.
- [13] R. Squitti, C. Salustri, M. Rongioletti and M. Siotto, *Front. Neurol.*, **2017**, *8*, 503.
- [14] P. Faller and C. Hureau, *Chem. Eur. J.*, **2012**, *18*, 15889-15889.
- [15] (a) J.L. Arbiser, S.K. Kraeft, R. van Leeuwen, S.J. Hurwitz, M. Selig, G.R. Dickersin, A. Flint, H.R. Byers and L.B.Chen, *Mol Med.*, **1998**, *4*(10), 665-670; (b) M. K. Lawson, M. Valko, M. T. D. Cronin and K. Jomová, *Curr. Pharmacol. Reports*, **2016**, 271-280.
- [16] (a) Y. Kwon and T. Kodadek, *J. Am. Chem. Soc.*, **2007**, *129*(6), 1508-1509; (b) J. Schwochert, R. Turner, M. Thang, R.F. Berkeley, A. R. Ponkey, K. M. Rodriguez, S. S. F. Leung, B. Khunte, G. Goetz, C. Limberakis, A.S. Kalgutkar, H. Eng, M. J. Shapiro, A. M. Mathiowetz, D. A. Price, S. Liras, M. P. Jacobson and R. Scott Lokey, *Org. Lett.*, **2015**, *17*(12), 2928-2931; (c) A. Furukawa, C. E. Townsend, J. Schwochert, C. R. Pye, M. A. Bednarek, and R. Scott Lokey, *J. Med. Chem.*, **2016**, *59*(20), 9503-9512; (d) N.C. Tan, P. Yu, Y.U. Kwon, T. Kodadek, *Bioorg. Med. Chem.*, **2008**, *16*(11), 5853-5861.
- [17] J. Seo, B.-C. Lee and R.N. Zuckermann in *Comprehensive Biomaterials Vol.2* (eds: ed. P. Ducheyne, K.E. Healy, D.W. Hutmacher, D.W. Grainger, C.J. Kirkpatrick), Elsevier, **2011**, pp. 53-76
- [18] R. N. Zuckermann, J. M. Kerr, W. H. Moosf and S. B. H. Kent, *J. Am. Chem. Soc.*, **1992**, *114*, 10646-10647.
- [19] R. J. Simon, R. S. Kania, R. N. Zuckermann, V. D. Huebner, D. A. Jewell, S. Banville, S. Ng, L. Wang, S. Rosenberg and C. K. Marlowe, *Proc. Natl. Acad. Sci. U. S. A.*, **1992**, *89*(20), 9367-9371.
- [20] (a) K. Kirshenbaum, A. E. Barron, R. A. Goldsmith, P. Armand, E. K. Bradley, K. T. V. Truong, K. A. Dill, F. E. Cohen, and R. N. Zuckermann, *Proc. Natl. Acad. Sci. U. S. A.*, **1998**, *95*, 4303-4308; (b) C. W. Wu, K. Kirshenbaum, T. J. Sanborn, J. A. Patch, K. Huang, K. A. Dill, R. N. Zuckermann and A. E. Barron, *J. Am. Chem. Soc.*, **2003**, *125*, 13525-13530; (c) J. R. Stringer, J. A. Crapster, Guzei, I. A. and H. E. Blackwell, *J. Am. Chem. Soc.*, **2011**, *133*, 15559-15567; (d) J.A. Crapster, I.A. Guzei and H.E. Blackwell, *Angew. Chem. Int. Ed.*, **2013**, *52*, 5079-5084; (e) O. Roy, G. Dumonteil, S. Faure, L. Jouffret, A. Kriznik and C. Taillefumier, *J. Am. Chem. Soc.*, **2017**, *139*, 13533-13540.
- [21] (a) J.T. Nguyen, C.W. Turck, F.E. Cohen, R.N. Zuckermann, W.A. Lim, *Science*, **1998**, *282*(5396), 2088-2092; (b) T. Hara, S. R. Durell, M. C. Myers and D. H. Appella, *J. Am. Chem. Soc.*, **2006**, *128*, 1995-2004; (c) D. G. Udugamasooriya, S. P. Dineen, R. A. Brekken and T. A. Kodadek, *J. Am. Chem. Soc.*, **2008**, *130*, 5744-5752.
- [22] (a) B. C. Lee, T. K. Chu, K. A. Dill and R. N. Zuckermann, *J. Am. Chem. Soc.*, **2008**, *130*, 8847-8855; (b) G. Maayan, M. D. Ward and K. Kirshenbaum, *Chem. Commun.*, **2009**, 56-58; (c) A. D'Amato, P. Ghosh, C. Costabile, G. Della Sala, I. Izzo, G. Maayan and F. De Riccardis, *Dalton Trans.*, **2020**, *49*, 6020-6029; (d) P. Ghosh and G. Maayan, *Chem. Sci.*, **2020**, *11*, 10127-10134; (e) P. Ghosh and G. Maayan, *Chem. - A Eur. J.*, **2021**, *27*, 1383.
- [23] (a) G. Maayan, M. D. Ward and K. Kirshenbaum, *Proc. Natl. Acad. Sci. U. S. A.*, **2009**, *106*, 13679-13684; (b) G. Della Sala, B. Nardone, F. De Riccardis and I. Izzo, *Org. Biomol. Chem.*, **2013**, *11*, 726-731; (c) R. Schettini, B. Nardone, F. De Riccardis, G. Della Sala & I. Izzo, *European J. Org. Chem.*, **2014**, 7793-7797; (d) K. J. Prathap and G. Maayan, *Chem. Commun.*, **2015**, *51*, 11096-11099; (e) R. Schettini, F. De Riccardis, G. Della Sala and I. Izzo, *J. Org. Chem.*, **2016**, *81*, 2494-2505; (f) C. M. Darapaneni, P. Ghosh, T. Ghosh and G. Maayan, *Chem. - A Eur. J.*, **2020**, *26*, 9573-9579.; (g) T. Ghosh, P. Ghosh and G. Maayan, *ACS Catal.*, **2018**, *8*, 10631-1064.
- [24] S. M. Miller, R. J. Simon, S. Ng, R. N. Zuckermann, J. M. Kerr, and W. H. Moos, *Drug Dev. Res.*, **1995**, *35*, 20-32.
- [25] (a) Y. Luo, S. Vali, S. Sun, X. Chen, X. Liang, T. Drozhzhina, E. Popugaeva and I. Bezprozvanny, *ACS Chem. Neurosci.*, **2013**, *4* (6), 952-962; (b) J. P. Turner, T. Lutz-Rechtin, K.A. Moore, L. Rogers, O. Bhave, M. A. Moss and S. L. Servoss, *ACS Chem. Neurosci.*, **2014**, *5*(7), 552-558; (c) K. Pradhan, G. Das, V. Gupta, P. Mondal, S. Barman, J. Khan, and S. Ghosh, *ACS Chem. Neurosci.*, **2019**, *10*(3), 1355-1368
- [26] M. Baskin and G. Maayan, *Chem. Sci.*, **2016**, *7*, 2809-2820.
- [27] C. M. Darapaneni, P. J. Kaniraj and G. Maayan, *Org. Biomol. Chem.*, **2018**, *16*, 1480-1488.

- [28] (a) Z. Xiao and A. G. Wedd, *Nat. Prod. Rep.*, **2010**, *27*, 768–789; (b) L. Zhang, M. Koay, M. J. Maher, Z. Xiao and A. G. Wedd, *J. Am. Chem. Soc.*, **2006**, *128*, 5834–5850
- [29] B. Alies, I. Sasaki, O. Proux, S. Sayen, E. Guillon, P. Faller and C. Hureau, *Chem. Commun.*, **2013**, *49*, 1214–1216
- [30] S. Chassaing, F. Collin, P. Dorlet, J. Gout, C. Hureau and P. Faller, *Curr. Top. Med. Chem.*, **2012**, *12(22)*, 2573–2595.
- [31] C. Hureau, *Coord. Chem. Rev.*, **2012**, *256*, 2164–2174.
- [32] J. T. Pedersen, S. W. Chen, C. B. Borg, S. Ness, J. M. Bahl, N. H. H. Heegaard, C. M. Dobson, L. Hemmingsen, N. Cremades and K. Teilum, *J. Am. Chem. Soc.*, **2016**, *138 (12)*, 3966–3969
- [33] (a) M. Miller, Q. W. Tejas, P. Telivala, R. J. Smith, A. Lanzirotti and J. Miklossy, *J. Struct. Biol.*, **2006**, *155(1)*, 30–37; (b) A. Conte-Daban, B. Boff, A. Candido Matias, C. N. M. Aparicio, C. Gateau, C. Lebrun, G. Cerchiaro, I. Kieffer, S. Sayen, E. Guillon, P. Delangle and C. Hureau, *Chem. – A Eur. J.*, **2017**, *23*, 17078.
- [34] V. B. Kenche, I. Zawisza, C. L. Masters, W. Bal, K. J. Barnham, and S. C. Drew, *Inorg. Chem.*, **2013**, *52 (8)*, 4303–4318
- [35] D. Yugay, D. P. Goronzy, L. M. Kawakami, S. A. Claridge, T.-B. Song, Z. Yan, Y.-H. Xie, J. Gilles, Y. Yang, and P. S. Weiss, *Nano Letters*, **2016**, *16(10)*, 6282–6289.
- [36] S. C. Drew and K. J. Barnham, *Acc. Chem. Res.*, **2011**, *44 (11)*, 1146–1155.